Available online at www.sciencedirect.com
SCIENCE DIRECT®
Journal of Photochemistry and Photobiology A: Chemistry 171 (2005) 9–20
Journal of Photochemistry and Photobiology A:Chemistry
www.elsevier.com/locate/jphotochem

Spectral characteristics of various prototropic species of 2-(3′-aminophenyl)pyrido[3,4-d]imidazole

Manoj K. Nayak, Sneh K. Dogra*

Department of Chemistry, Indian Institute of Technology Kanpur, Kanpur 208 016, India

Received 6 May 2004; received in revised form 21 July 2004; accepted 24 August 2004
Available online 30 November 2004

Abstract

Spectral characteristics of the prototropic species of 2-(3′-aminophenyl)pyrido [3,4-d]imidazole (3-APPI) have been studied in three non-aqueous and aqueous solvents, using absorption, fluorescence excitation and fluorescence spectroscopy, as well as, time dependent spectrofluorimetry. Acid concentration in ether is controlled by trifluoroacetic acid (TFA), whereas in other three solvents H_2SO_4 is used. Semi-empirical quantum mechanical calculations (AM1) and density functional theory (DFT) calculations have been carried out on all kinds of neutral and ionic species. Combining the experimental and theoretical results, the spectral characteristics have been assigned to various cationic and monoanionic species. It has been shown that: (i) only one kind of monoanion (MA) is formed by the deprotonation of >N−H moiety and one kind of trication (TC), (ii) two kinds of monocations (MC1 and MC3) in the ground (S_0) and first excited singlet (S_1) states in polar aprotic and protic solvents, whereas only one monocation (MC3) is formed in ether + TFA system. pK_a values for the various prototropic reactions were determined in S_0 and S_1 states and discussed.

Keywords: 2-(3′-Aminophenyl)pyrido-[3,4-d]imidazole; Absorption spectrum; Fluorescence spectrum; Acid–base equilibrium; Theoretical calculations

1. Introduction

It is well established that the photophysical and spectral characteristics of aromatic hydrocarbons are not only sensitive to the nature of substituents, but also to the position of the substituent and especially if these are more than 1 [1–3]. For example the photophysical properties of 1,2-, 1,3- and 1,4-diaminobenzenes (1,2-DAB, 1,3-DAB, 1,4-DAB) [4], different diamino derivatives of naphthalenes [5,6] are not only different with respect to each other but their sensitivity to solvent polarity and hydrogen bond forming tendency is also different. Thus these molecules and many other similar molecules can act as very good probes for the characterization of macro- or biomolecules [7].

Other property, which is also affected by the position of substituent, is the acid–base character. It is well established now that acidity and basicity of these centers changes drastically on excitation to S_1 state [2,3,8,9]. Many parameters have been used to establish the nature of ionic species (e.g. total energy obtained by AM1 method, DFT, etc.) and to correlate the changes in the acidity or basicity of these centers. For example, charge densities at different basic centers in S_0 and S_1 states, effective valence electron potential [10–12], electrostatic potential energy mapping [13], etc. Experimental results have shown that the pK_a values for the protonation of benzimidazole (BI) and indazole are 5.67 and 1.26, respectively, in S_0 state when the protonation site is the same (–N= atom) [14,15]. Many such examples are there in literature [5,6,8,16–20].

For more than two decades, our group is actively involved in synthesizing and studying the photophysical behavior of *N*-heterocyclic aromatic molecules as a function of solvent and acid–base concentration [21–25]. In our recent study on 2-(4′-*N*,*N*-dimethylaminophenyl)pyrido[3,4-d]imidazole (2-DMAPPI) [26,27], we have shown the presence of one kind of monoanion (MA1) and trication (TC), two kinds of monocations (MC1 and MC3) in S_0 state and (MC2 and MC3)

* Corresponding author. Tel.: +91 512 597 163; fax: +91 512 597 436.
E-mail address: skdogra@iitk.ac.in (S.K. Dogra).

1010-6030/$ – see front matter © 2004 Elsevier B.V. All rights reserved.
doi:10.1016/j.jphotochem.2004.08.021

in S_1 state and three kinds of dications (DC1–DC3). It was also established that MC2 in S_1 state formed was from MC1, by transferring proton of $-NH^{\oplus}Me_2$ moiety to $=N^8-$ atom of imidazole involving solvent molecules. Moreover, proportion of different DCs depends upon the nature of the solvent.

In continuation to our earlier work, the present study on 3-APPI has been carried out from following angles. (i) It has been established earlier that 3′-amino derivative of 2-(aminophenyl)benzazoles (benzimidazole, BI; benzoxazole, BO; benzothiazole, BT) are very polar and sensitive to solvents in S_1 state as compared to 2′- and 4′-aminophenyl derivatives [28–32]. Thus 3-APPI will also be having similar behavior and thus can be used as probe molecule. (ii) Basic centers ($=N^2-$, $=N^8-$ and $-NH_2$) present in 3-APPI are also similar to those present in DMAPPI [27]. Similar behavior is also expected from 3-APPI when acid–base concentrations are changed. In order to confirm the above-mentioned facts, absorption, fluorescence and fluorescence excitation spectroscopy, as well as, time dependent spectrofluorimetry have been used. Characterization of various ionic species have been carried out by doing electronic structure calculations using semi-empirical AM1 method and DFT procedure using Gaussian'98 program. Three different solvents (ether, acetonitrile and methanol) have been used to assign and characterize the cationic species. Trifluoroacetic acid (TFA) has been used in ether to maintain acid strength, whereas H_2SO_4 has been used in other solvents. Cyclohexane as nonpolar solvent could not be used because of the insolubility of 3-APPI.

2. Materials and methods

3-APPI was prepared from 3,4-diaminopyridine and 3-aminobenzoic acid by the procedure reported in literature [33]. 3-APPI was purified by repeated crystallization from methanol. Purity of 3-APPI was checked by using different spectroscopic techniques, as well as, by verifying that the fluorescence excitation spectrum was identical when the emission was monitored at different wavelengths (λ_{em}). Solvents used were either of spectroscopic grade or HPLC grade from E. Merck and were used as-received. All the solvents were checked for spurious fluorescence in the region of fluorescence measurements. Triply distilled water was used for aqueous solutions. Analytic grade H_2SO_4, NaOH and *o*-phosphoric acid (all from E. Merck) were used as-received.

Aqueous solutions in the pH range of 3–11 were prepared by mixing appropriate amounts of dilute ($\sim 10^{-3}$ M) solutions of NaOH and *o*-H_3PO_4. Hammett's acidity scale (H_0) [34] was used in preparing aqueous solutions of pH < 1.0 and Yagil's basicity scale (H_-) [35] was used in preparing aqueous solutions of pH > 13. All the spectral measurements were carried out at the solute concentrations of the order of $\sim 10^{-5}$ M. Fluorescence quantum yields (Φ_f) were determined for solutions having absorbance less than 0.1 at the excitation wavelengths (λ_{ex}) and referred to quinine sulphate in 1 N H_2SO_4 ($\Phi_f = 0.55$) [36]. For fluorimetric titrations, the solutions were excited at the isosbestic wavelengths of the absorption spectra, i.e. 285 and 305 nm for dication–monocation (DC–MC), 305 and 328 nm for the monocation–neutral (MC–N) and 288 and 330 nm for neutral–monoanion (N–MA) equilibria. Instruments used for recording absorption, fluorescence and fluorescence excitation and excited state lifetime measurements are the same as described in our recent publication [37].

3. Theoretical calculations

Scheme 1 shows the various MCs (MC1–MC3), DCs (DC1–DC3) and MAs (MA1 and MA2) considered for theoretical calculations. S_0 and S_1 states parameters (total energy as compared to the most stable species *E*, dipole moments, μ_g and μ_e, dihedral angle (φ, $C_{11}C_{10}C_9N_7$), charge densities at the respective basic centers of neutral) of each species of 3-APPI were obtained by optimizing the geometries in the respective state using the AM1 method (QCMP 137, MOPAC 6/PC) and coordinates obtained from PCMODEL [38,39]. In S_1 state, configuration interactions (CI = 5 in MOPAC, 100 configurations) were considered to optimize the geometry. Transition energies for absorption and emission processes were obtained by carrying out standard single point calculations in AM1 method and using S_0 and S_1 state geometries, respectively. Relevant data are compiled in respective tables. Transition energies were also obtained by using CNDO/S-CI method [40,41], as described in our recent paper [37] and are given in Table 1. Dipolar solvation energies for different species in S_0 and S_1 states were calculated using the following expression, based on Onsager's theory [42]:

$$\Delta E_{solv} = -\left(\frac{\mu^2}{a^3}\right) f(D)$$

where $f(D) = (D-1)/(2D+1)$, D is the dielectric constant of the medium, μ the dipole moment of the respective state and a the Onsager's cavity radius. For non-spherical molecule, like 3-APPI, value of a was obtained by taking 40% of the maximum length of the molecule [43] and is 0.488 nm.

The electronic structure calculations were also performed on each species as mentioned in Scheme 1, using Gaussian'98 program [44]. The geometry optimization was performed on each species of 3-APPI in S_0 state using DFT [45,46] B3LYP with 6-31G** basis set [44,47]. Geometry of these stationary points on S_1 state was calculated using configuration interaction singles (CIS) [48] theory with 6-31G** basis sets. Time dependent (TD) DFT [49,50] B3LYP was also used to calculate the excited state energies at calculated stationary point geometry in S_0 and S_1 states. Relevant data are compiled in Tables 1 and 2, respectively.

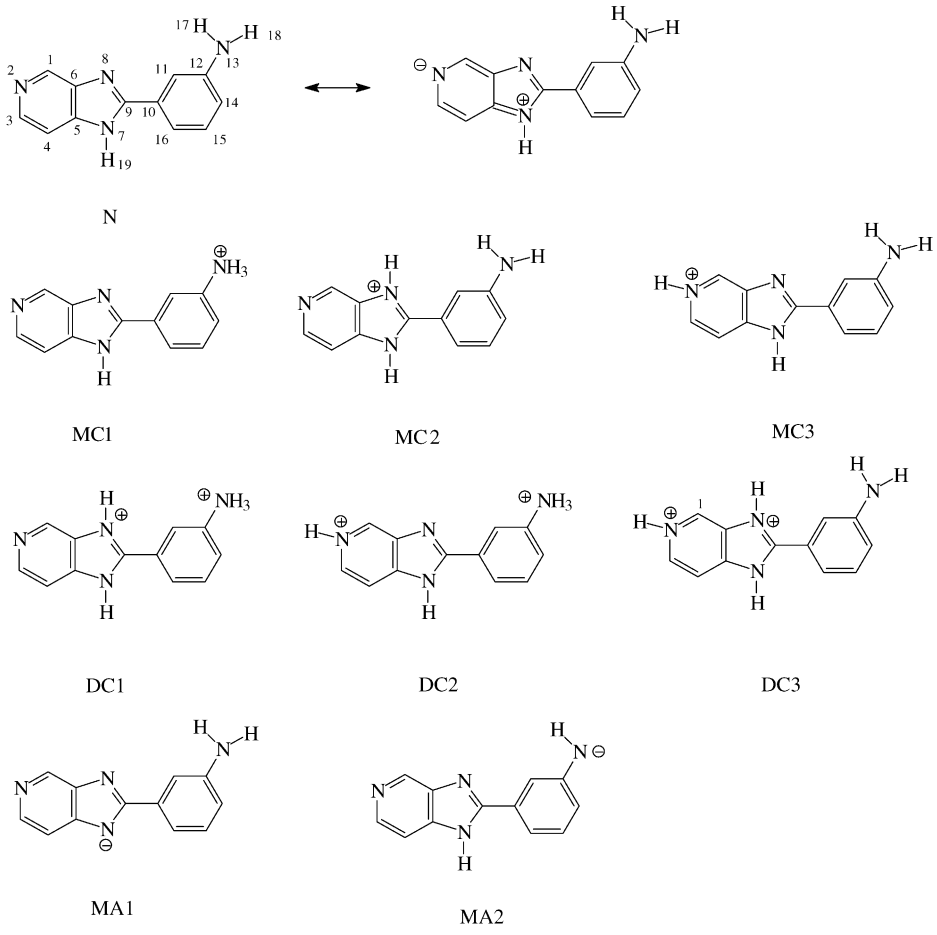

Scheme 1.

4. Results and discussion

4.1. Effect of solvents

Absorption band maximum (λ^{ab}_{max}) and molecular extinction coefficients ($\log \varepsilon_{max}$) of 3-APPI in different solvents are compiled in Table 3, except for cyclohexane. Absorption spectrum in each solvent consists of three bands, i.e., ~254 nm of medium intensity, ~288 nm of maximum intensity and a shoulder (sh) at ~326 nm. All the λ^{ab}_{max} are red shifted with respect to 2-phenylbenzimidazole (2-PBI) [51], but are at the similar λ^{ab}_{max} when compared with 3-APBI [28], 3-APBO [31] and 3-APBT [32]. This suggests that presence of =N– in the benzo ring of BI does not affect the absorption spectral characteristics of these molecules, except the band shape and absorbance. A similar comparison is observed between benzene and pyridine. Red shift observed in λ^{ab}_{max} of 3-APPI in comparison to 2-PBI is due to the resonance effect of $-NH_2$ group lone pairs. Hardly any change observed in these λ^{ab}_{max} with change in polarity or protic nature of solvents suggests very weak interactions with the solvents, which is also supported by full width at half the maximum height (FWHM) that is nearly constant in all the solvents ($4860 \pm 100\,cm^{-1}$). Similar behavior is observed for different benzimidazoles [14] and 2-(4′-aminophenyl)pyrido[3,4-d]imidazole (4-APPI) [20] and many other systems. Similar to 2-APPI [20], BIs and 4-APPI [20], 3-APPI has three basic centers and can form hydrogen bonding. If π, π^* is the lowest energy transition, interactions with $=N^2-$ and $=N^8-$ atoms will lead to red shifts and with $-NH_2$ group will lead to blue shifts in the spectral characteristics. If more than one basic center is present and effect of interactions is acting in opposite directions, complicacies or irregularities arise. The net effect will be either reduced or cancelled. The present molecule belongs to this class of molecule and thus the net effect of solvents negligible.

Fluorescence band maximum (λ^{ab}_{max}) and Φ_f in different solvents are compiled in Table 3. Unlike absorption spectrum, fluorescence spectrum is very sensitive to solvent polarity and protic nature. Thus it is consistent with the behavior of aromatic amines in S_1 state that greater charge transfer takes place from amino group to aromatic ring in S_1 state than that in S_0 state. This is supported by increase of dihedral angle (φ) from 160° to 178° and decrease of C_9–C_{10} bond length from 0.1466 to 0.1417 nm when excited to S_1 state. This is also supported by the fact that FWHM of the emission band

Table 1
Calculated properties of 3-APPI [neutral (N), monocations (MCs)] in the ground and excited singlet states

Characteristics	N	MC1	MC2	MC3
S_0 stage				
AM1 method				
E (kJ mol^{-1})	−2500.1093[a]	74.3	0.0	9.2
E_{sol} (kJ mol^{-1})	−2500.1747[a]	0.0	45.0	18.4
μ_g (D)	4.4	9.0	2.1	10.8
DFT B3LYP				
E (kJ mol^{-1})	−682.3406[b]	120.5	29.7	0.0
μ_g (D)	5.35	19.24	3.83	8.20
S_1 stage (F.O.G.)				
AM1 method				
E (kJ mol^{-1})	−2496.5631[a]	132.3	20.6	0.0
E_{sol} (kJ mol^{-1})	−2496.6224[a]	130.1	9.4	0.0
μ_e (D)	4.19	7.69	9.38	7.4
Transition energies (nm) (oscillator strength); absorption				
CNDO/S-CI method				
S_0–S_1	300 (0.38)	346.7 (0.39)	345.5 (0.18)	335 (0.07)
S_0–S_2	278.8 (0.05)	327.8 (0.02)	316.4 (0.14)	318.4 (0.14)
TD (DFT) method				
S_0–S_1	322.3 (π, π^*) (0.069)	375 (n, π^*) (0.0000)	439.4 (π, π^*) (0.059)	576.8 (π, π^*) (0.024)
S_0–S_2	283.6 (π, π^*) (0.556)	359 (π, π^*) (0.2661)	321.7 (n, π^*) (0.0005)	452 (π, π^*) (0.009)

[a] Energy in eV.
[b] Energy in Hartree.

in any respective solvent is smaller than that observed in the long wavelength (LW) band of absorption spectrum. As mentioned above, this is due to loss of flexibility of the molecule in S_1 state. An increase in the Stokes shift with increase of solvent polarity and protic nature confirms the increase of delocalization of lone pair of amino group throughout the aromatic moiety in S_1 state. Φ_f of 3-APPI is greater than that of 1,3-DAB [4] and 3-APBI [28] in any respective solvent. Similar to these molecules, Φ_f of 3-APPI also decreases when the polarity and protic nature of the solvents is increased. Similar λ^f_{max} observed at different λ_{ex} suggests that emission is occurring from the lowest and most relaxed electronically excited state, in agreement with Kasha's rule [52], even though 3-APPI is excited to different electronically states. On the other hand, a definite increase in the Φ_f (nearly 55–60% in each solvent) is observed when λ_{ex} is increased from 290 to 330 nm. This could be due to the competition between the rate of intersystem crossing from higher singlet states to triplet states and the rate of emission. Similar behavior is also observed in 2-aminofluorene [53] and 2-hydroxyquinoxaline [22].

Table 2
Calculated properties of 3-APPI [dications (DCs) and monoanions (MAs] in ground and excited singlet states

Characteristics	DC1	DC2	DC3	MA1	MA2
S_0 state					
AM1 method					
E (kJ mol^{-1})	62.6	0.0	65.2	0.0	89.1
E_{sol} (kJ mol^{-1})	0.0	28.2	62.9	0.0	58.8
μ_g (D)	17.3	6.6	11.9	7.8	11.8
DFT method					
E (kJ mol^{-1})	103.7	0.0	35.7	0.0	106.1
μ_g (D)	17.6	7.2	9.1	8.7	11.4
S_1 state					
AM1 method					
E (kJ mol^{-1})	210.7	189.4	0.0	78.1	0.0
E_{sol} (kJ mol^{-1})	152.0	167.4	0.0	84.1	0.0
μ_e (D)	13.2	8.1	3.3	1.8	4.3
Transition energies (nm)					
CNDO/S-CI method; absorption					
S_0–S_1	325	302	465	349	459
S_0–S_2	288	289	344	317	341
TD (DFT) method; absorption					
S_0–S_1	407	285	817	325	852.0
S_0–S_2	345	275	524	305	542.0
Emission					
S_1–S_0	432	377	1244	–	–

Fluorescence excitation spectra of 3-APPI observed in each solvent and at different λ_{em} are similar to each other and also resembled with the absorption spectrum of 3-APPI in that solvent. This suggests that there is only one species in S_0 state and emission is taking place from the state, which is excited. Excited singlet state lifetimes were measured by using exciting wavelength, λ_{exc} = 337 nm and monitoring at the λ^f_{max} in the respective solvent. Fluorescence decay profile in each case followed a single exponential with $\chi^2 = 1 \pm 0.1$ and good autocorrelation function. Values of radiative (k_r) and non-radiative ($k_{nr} = k_{ic} + k_{isc}$, where k_{ic} and k_{isc} are the rate constants for internal conversion and intersystem crossing, respectively) rate constants were calculated from the fol-

Table 3
Absorption band maxima (λ^{ab}_{max}, nm), log ε_{max}, fluorescence band maxima (λ^{f}_{max}, nm), fluorescence quantum yield (Φ_f) of APPBI in different solvents, [3-APPI] = 8.95×10^{-6} M and ionic species, [3-APPI] = 1.3×10^{-5} M

Solvents	λ^{ab}_{max} (log ε_{max})			λ^{f}_{max} (Φ^f) at λ_{exc} = 290 nm	λ^{f}_{max} (Φ^f) at λ_{exc} = 330 nm
Ether	254 (4.181)	289 (4.276)	326 (3.639)	392 (0.147)	392 (0.236)
Dioxane	255 (4.235)	288.5 (4.353)	327 (3.729)	395 (0.15)	395 (0.251)
Ethyl acetate	254 (4.172)	289 (4.286)	327 (3.681)	401.6 (0.155)	401.6 (0.233)
Acetonitrile	253 (4.233)	288.5 (4.327)	327 (3.729)	411 (0.167)	411 (0.259)
Iso-propanol	–	289 (4.378)	328 (3.691)	436 (0.22)	435.5 (0.36)
Methanol	–	288 (4.364)	327 (3.691)	438.5 (0.023)	438.5 (0.037)
Water					
pH 8.5	–	288 (4.339)	325 sh	458 (0.0013)	458 (0.002)
pH 5.3	252 sh	292 (4.297)	340 (3.634)	359, 450 (0.0066, 0.0004)	455 ± 5 (0.0005)
pH 1.0	239 (4.506)	286 (4.340)	–	314, 327.5, 343, 359, 380 (0.0195)	–
pH 12.0	–	295 (4.348)	–	407 (0.00055)	420 (0.0009)
H_- = 16.0	–	298 (4.339)	–	401 (0.0006)	417 (0.00093)
H_0 = −3.5	243 (4.295)	290 (4.405)	308 sh	330,344 (0.00005)	–
H_0 = −10.0	244 (4.296)	291 (4.415)	309 sh	346.5 (0.0014)	–

lowing relationships:

$$k_r = \frac{\Phi_f}{\tau}, \qquad k_{nr} = \frac{1}{\tau - k_r}$$

and are compiled in Table 4. Values of k_r ($5.0 \pm 0.3 \times 10^7\ s^{-1}$) and k_{nr} ($15.3 \pm 2 \times 10^7\ s^{-1}$) are nearly constant in polar aprotic solvents, but decrease and increase, respectively, very sharply in polar protic solvents. It is well established that rates of non-radiative processes decrease with the loss of flexibility [54] of the molecule. 3-APPI, as mentioned above, is less flexible in S_1 state as compared to that in S_0 state. Thus values of k_{nr} should decrease. This is not observed in polar protic solvents. It can be concluded that increase in the non-radiative rate constant is due to solvent induced fluorescence quenching. Similar examples are presented in literature [21b,53,55].

Sensitivity of fluorescence spectrum to solvent polarity can be measured by Stokes shift and variation of Stokes shifts with solvent polarity can be represented by many equations. We are using the BK equation (2) to correlate Stokes shift with solvent polarity and to calculate the value of μ_e, provided μ_g is known:

$$\bar{\nu}_{ss} = \bar{\nu}_{ab} - \bar{\nu}_{fl} = m_1 f(D, n) + \text{const.} \quad (2)$$

$$m_1 = \frac{(\mu_e - \mu_g)^2}{\beta a^3} \quad (3)$$

where $\beta = 2\pi\varepsilon_0 hc = 1.105 \times 10^{-35}\ C^2$. In case of isotropic polarizability of molecules, the condition $2\alpha/4\pi\varepsilon_0 a^3 = 1$ is frequently satisfied and Eq. (2) will represent BK equation. When $\alpha = 0$ (polarizability is neglented), Eq. (2) reduces to Eq. (4), derived by Lippert [56] and Mataga et al. [57]:

$$\bar{\nu}_{ss} = \bar{\nu}_{ab} - \bar{\nu}_{fl} = m_1 \left[\frac{D-1}{2D+1} - \frac{n^2-1}{2n^2+1}\right] + \text{const.} \quad (4)$$

BK polarity parameters for $\alpha = 0$ and $\alpha = 1$ have been taken from the literature [58]. Plot of Stokes shifts versus BK parameters for $\alpha = 0$ and $\alpha = 1$ for polar aprotic solvents is linear, whereas large departure from linearity is observed for polar protic solvents. Similar behavior is also observed for aromatic

Table 4
Excited state lifetimes (τ, ns), fluorescence quantum yields (Φ_f), radiative (k_r, $\times 10^7\ s^{-1}$) and non-radiative (k_{nr}, $\times 10^7\ s^{-1}$) rate constants of 3-APPI in different solvents

Solvents	λ^{f}_{max} (Φ_f) at λ_{exc} = 330 nm	τ/χ^2	k_r	k_{nr}
Ether	392 (0.236)	4.31 (1.0)	5.48	17.72
Dioxane	395 (0.251)	5.23 (1.09)	4.80	13.89
Ethyl acetate	401.6 (0.233)	4.76 (1.09)	4.90	16.1
Acetonitrile	411 (0.259)	5.52 (1.04)	4.70	13.41
Iso-propanol	435.5 (0.36)	10.52 (1.15)	3.42	6.08
Methanol	438.5 (0.037)	1.38 (1.08)	2.68	69.78
pH 8.5	458 (0.002)	0.31 (1.12)	0.64	321.94
pH 5.3	450 ± 5 (0.0006)	–	–	–
pH 1.0[a]	314, 327.5 (0.0229), 343, 359, 380	0.71 (0.90)	3.23	137.61
pH 12.0	420 (0.0009)	–	–	–
H_- = 16.0	417 (0.00093)	–	–	–
H_0 = −3.5[a]	329, 346 (0.00009)	–	–	–
H_0 = −10.0[a]	446 (0.0022)	0.75 (0.90)	0.29	133.04

[a] Mean quantum yields are obtained at λ_{exc} = 305 nm for these solutions.

amines in these solvents and thus can be explained in a similar manner [21,53,59,60]. This is supported by the linear plot of Stokes shift versus $E_T(30)$ parameters, which also includes the specific interaction. If protic solvents are excluded, the regression coefficients observed for BK parameters for $\alpha = 0$ and $\alpha = 1$ are 0.98 and 0.99, respectively. Thus it is not possible to draw any conclusion about whether polarizability of the fluorophore plays a role or not in finding out μ_e.

μ_e was determined from the slope of the linear part of the plots (not shown) using μ_g obtained from AM1 method or by DFT calculations and value of Onsager's cavity radius as 0.488 nm. Values of μ_e obtained for $\alpha = 0$ and $\alpha = 1$ are found to be 8.0 and 6.33 D respectively, suggesting that μ_e is a function of polarizability of the fluorophore. Results of Table 1 suggest that values of μ_e obtained by AM1 method or from CNDO/S-CI calculations agree better with the results when polarizability of the fluorophore is included. In other words polarizability plays a major role in increasing the value of μ upon excitation to S_1 state. Small discrepancy observed between the experimental and calculated results is due to the assumption that polarizability is isotropic.

4.2. Effects of acid–base concentration

As shown in Scheme 1, 3-APPI possesses two acidic centers (–NH_2, >N–H) and three basic centers (–NH_2, =N^2–, =N^8–). Thus there can be two MAs (MA1 and MA2), three MCs (MC1–MC3), three DCs (DC1–DC3) and only one trication (TC). Thus the prototropic equilibrium for each conjugate acid–base pair will be considered separately. pK_a values for different prototropic equilibria were determined in the ground (pK_a) and first excited singlet state (pK_a^*) and are depicted in Scheme 2.

4.2.1. Monoanion

λ_{max}^{ab} of neutral species of 3-APPI (N) at 287 nm is red shifted to 295 nm with nearly similar absorbance, whereas λ_{max}^{ab} at 325 (sh) is blue shifted with increase in absorbance. Isosbestic points observed at 332 and 288 nm in the pH range of 8–12.50 suggest the presence of equilibrium between N–MA. No further change is observed in the λ_{max}^{ab} with increase of base concentration up to $H_- = 16$ except slight increase in the width of absorption spectrum at $H_- = 16$. pK_a value obtained from absorption data for N–MA equilibrium is 10.20. Fluorescence spectrum of 3-APPI is blue shifted from 458 to 407 nm when excited at $\lambda_{exc} = 288$ and 332 nm under basic conditions. Similar to absorption spectrum, no change in λ_{max}^{f} and fluorescence intensity is observed up to $H_- = 16$. Fluorescence excitation spectra recorded at pH 12.5 and $H_- = 16$, and monitoring at different λ_{em} resemble with each other and with absorption spectra, suggesting that species in S_0 and S_1 states are similar. Excited state pK_a (pK_a^*) value for N–MA equilibrium was determined by fluorimetric titration method using λ_{exc} as λ_{isos} (332 nm). Value so obtained is similar to the ground state pK_a value (10.25). pK_a and pK_a^* values obtained are less than the similar deprotonation constant of 2-PBI (11.5) [51] and 3-APBI (11.9) [60].

Results of Table 2 suggest that MA1 is more stable than MA2 by 89.1 and 58.8 kJ mol^{-1}, respectively, under isolated conditions and when dipolar solvation energy is included and using AM1 calculations, whereas DFT calculations indicate that MA1 is stable by 106 kJ mol^{-1}. Thus in S_0 state only MA1 is present in the system and spectral characteristics can be discussed by taking this as the species. In general, deprotonation of >N–H group leads to red shift in the absorption and fluorescence spectra. This is contrary to the results mentioned above. It can be explained as follows. Charge transfer from –NH_2 group is only localized on phenyl ring, whereas resonance structure on PI ring is given in Scheme 1. It is clear from the resonance structure that charge density will decrease at >N–H and makes it more acidic. The deprotonation constant (10.25) of >N–H moiety supports this resonance structure. Dissociation of >N–H moiety leaves a negative charge on PI ring, which is delocalized over the imidazole and pyrido ring due to resonating structure. This may decrease the coplanarity of pyrido and phenyl rings. On the other hand, AM1 calculations have shown that both PI and phenyl rings are better coplanar in MA than in neutral 3-APPI, whereas amino group in MA is less coplanar with phenyl ring than in neutral 3-APPI. As mentioned earlier, LW absorption band is localized on phenyl ring and perturbed by PI ring, whereas second band is localized on PI ring and perturbed by phenyl ring. Thus slight blue shift observed in LW absorption band

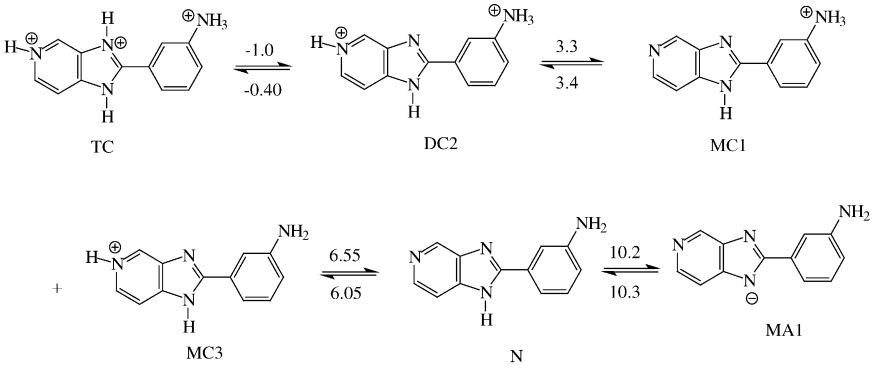

Scheme 2.

is due to decrease in the sharing of the lone pair of electrons of $-NH_2$ group with phenyl ring. Since emission is occurring from the lowest excited state, blue shift observed in emission spectrum of MA with respect to neutral species can be explained on the same lines. A similar behavior has also been observed in the deprotonation of >N–H group in 2-(4′-aminophenyl) and 2-(4′-hydroxyphenyl) benzimidazoles [30,61].

Excited state geometrical optimization including configuration interactions have shown that MA2 is more stable than MA1 by 78.1 and 84.1 kJ mol^{-1} under isolated conditions and when dipolar solvation energy is included. In other words when MA1 is excited to S_1 state proton transfer should take place from $-NH_2$ group to >N$^-$ moiety. This kind of excited state intramolecular proton transfer (ESIPT) does take place in many systems [21] but it involves the participation of the solvent molecules and should be complete during the lifetime of MA1. λ^{f}_{max} of the deprotonated species is large Stokes shifted. Further MA2 in general are non-fluorescent in nature with few exceptions [15]. Emission observed under basic conditions rules out this possibility and thus suggests that lifetime of MA1 may be too short to observe this kind of ESIPT. Ground state pK_a value observed from fluorimetric titrations for N–MA equilibrium supports this and suggests that the rates of deprotonation/protonation of the conjugate acid–base pair are slower than the rates of radiative decays of the corresponding species. It is thus concluded that MA2 is not formed in S_1 state even though AM1 calculations predict it.

4.2.2. Monocations

Absorption spectrum of 3-APPI was recorded in four solvents: ether + TFA up to 0.01 M (Fig. 1a), acetonitrile (Fig. 2a) and methanol + 1 M H_2SO_4 and water up to pH 5.3 and 8.5 (Fig. 3a). Absorption spectrum of 3-APPI at these acid concentrations is similar in all the solvents and relevant data are compiled in Tables 4 and 5. In all the cases both the absorption band systems are red shifted on acidification. Absorbance of both the red shifted λ^{ab}_{max} is less than those of the neutral species. Isosbestic points observed at 300 and 330 nm in the pH range of 4–8.5 suggest the presence of equilibrium between MC and neutral or between different MCs and

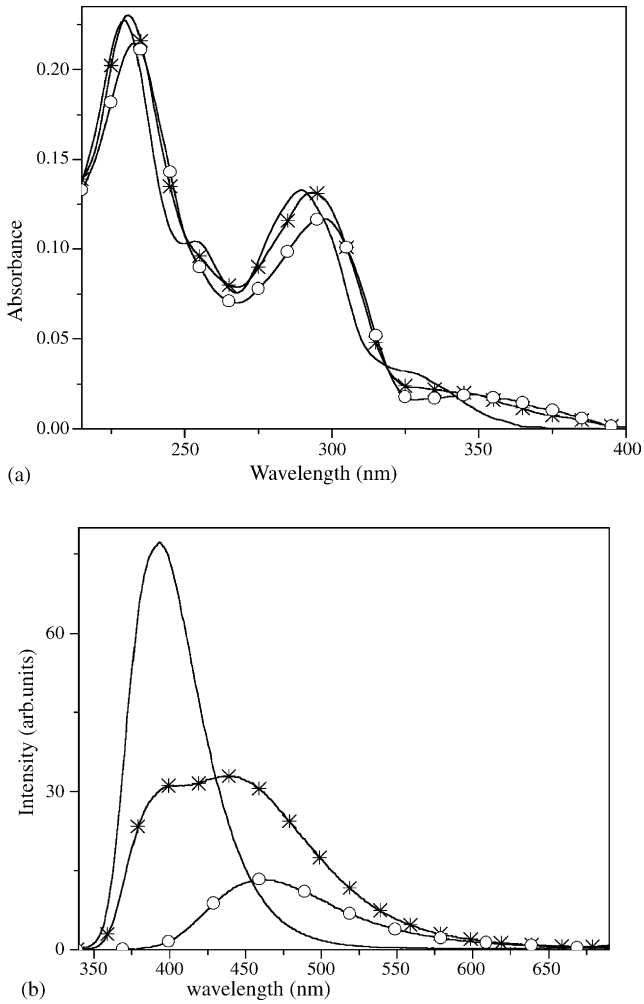

Fig. 1. (a) Absorption spectra of various ionic species of 3-APPI in ether + TFA: (—) 0 M TFA; (*) 10^{-3} M TFA; (◯) 0.1 M TFA. (b) Fluorescence spectra of various ionic species of 3-APPI in ether + TFA: (—) 0 M TFA; (*) 10^{-3} M TFA; (◯) 0.1 M TFA, at λ_{exc} = 338 nm.

neutral 3-APPI. pK_a value obtained for MC–N prototropic equilibrium, using Hendrickson equation, is found to be 6.55 with a slope of 0.95. pK_a value so obtained is greater than the similar prototropic equilibrium constants for any of the basic center (BI, BO, BT, pyridine, etc.) and 3-APBI (4.5) [60] but nearly similar to that noticed for DMAPPI (6.45) [27].

Table 5
Absorption band maxima (λ^{ab}_{max}, nm) and fluorescence band maxima (λ^{f}_{max}, nm) of 3-APPI in ether, acetonitrile and methanol containing different amounts of acid

Solvents	λ^{ab}_{max}			λ^{f}_{max}
Ether + 0 M TFA	254	289	326	392
Ether + 0.1 M TFA	–	297	350	462
Acetonitrile + 0 M H_2SO_4	253	288.5	327	411
Acetonitrile + 1 × 10^{-5} M H_2SO_4	240	293.5	350	316, 331, 345, 362, 438[a] (weak)
Acetonitrile + 1 × 10^{-4} M H_2SO_4	245	289	–	316, 331, 345, 362
Methanol + 0 M H_2SO_4	–	288	327	438
Methanol + 1 × 10^{-4} M H_2SO_4	–	294	350	316, 331, 344, 362, 382, 450[a] (weak)
Methanol + 0.1 M H_2SO_4	240	290	–	316, 331, 345, 362, 382

[a] λ_{exc} > 340 nm.

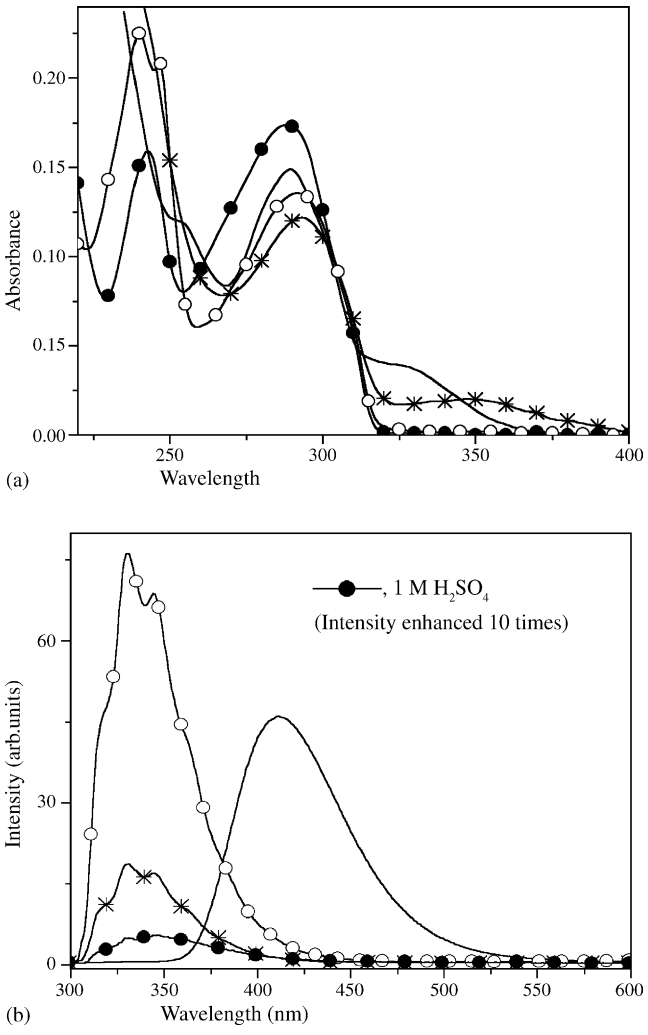

Fig. 2. (a) Absorption spectra of various ionic species of 3-APPI in acetonitrile + H_2SO_4: (—) 0 M H_2SO_4; (*) 10^{-5} M H_2SO_4; (◯) 10^{-4} M H_2SO_4; (●) 1 M H_2SO_4. (b) Fluorescence spectra of various ionic species of 3-APPI in acetonitrile + H_2SO_4: (—) 0 M H_2SO_4; (*) 10^{-5} M H_2SO_4; (◯) 10^{-4} M H_2SO_4; (●) 1 M H_2SO_4, at λ_{exc} = 302 nm.

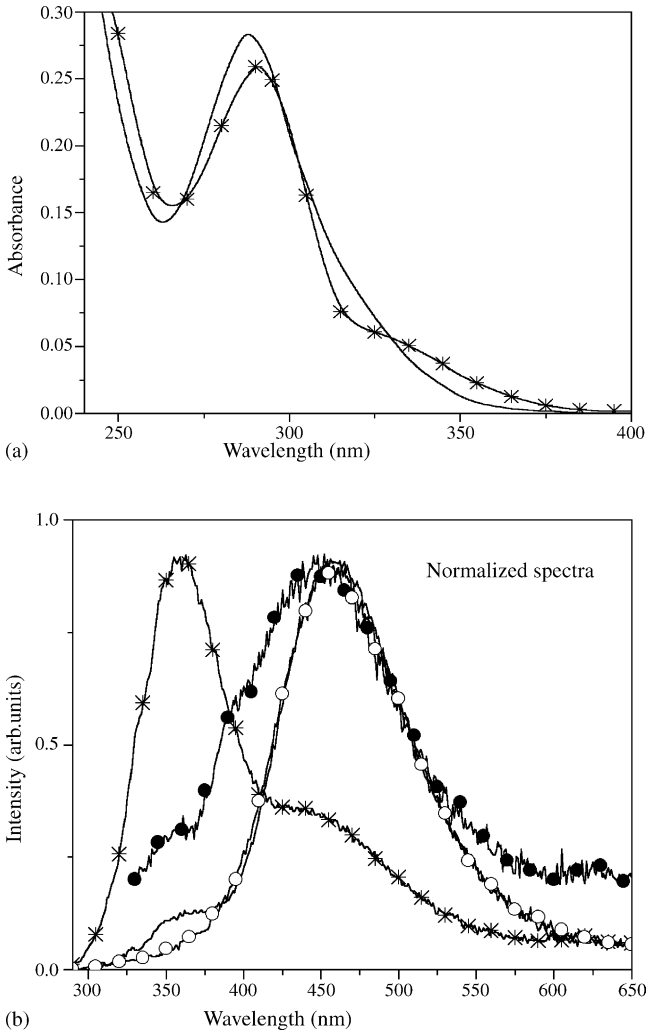

Fig. 3. (a) Absorption spectra of 3-APPI in water at: (—) pH 8.5; (*) pH 5.3. (b) Fluorescence spectra of 3-APPI in water at different excitation wavelengths: (—) pH 8.5; (*) pH 5.3, at λ_{exc} = 300 nm and (◯) pH 8.5; (●) pH 5.3, at λ_{exc} = 330 nm.

Fluorescence spectra of 3-APPI under the above acidic conditions in different solvents are more complicated than the absorption spectrum under similar conditions. In ether containing TFA > 10^{-3} M, large red shifted emission is observed at 462 nm and it is invariant to λ_{exc} (Fig. 1b). In all other three solvents and [H_2SO_4] ∼ 10^{-4} M, a structured emission band (Figs. 2b and 3b) is observed with $\nu_{vib} = 1340 \pm 60\ cm^{-1}$ at λ_{exc} < 320 nm. At λ_{exc} > 320 nm another weak emission band is observed at ∼450 nm. Fluorescence intensity of short wavelength (SW) emission band decreases and that of long wavelength (LW) emission band increases with increase of λ_{exc}. Fig. 3b represents the fluorescence spectra of 3-APPI under these acid conditions.

Fluorescence excitation spectra of 3-APPI under acidic conditions in different solvents were recorded at λ_{em} in the range of 350–500 nm. In ether containing 10^{-4} M TFA, fluorescence excitation spectrum is similar to each other when monitored at different λ_{em} and resemble with absorption spectra. This suggests the presence of only one species in S_0 state and emission is occurring from the same state to which it is excited. As the polarity and protic nature of the solvents increases, intensity of fluorescence excitation spectrum recorded at λ_{em} > 400 nm decreases, suggesting the presence of two species, one having the emission band in the range of 310–400 nm and one above 400 nm. This behavior is in agreement with that observed in DMAPPI [27]. Fig. 4 represents the fluorescence excitation spectra of 3-APPI in aqueous medium at pH 5.3. Excited states lifetimes of MCs could not be determined because of their poor fluorescence quantum yields.

As mentioned earlier, there can be three different kinds of MCs (MC1–MC3, Scheme 1). Fluorescence emission and excitation spectra suggest the presence of two MCs having different structures in aqueous medium. AM1 calculations suggest that the order of stability of MCs under

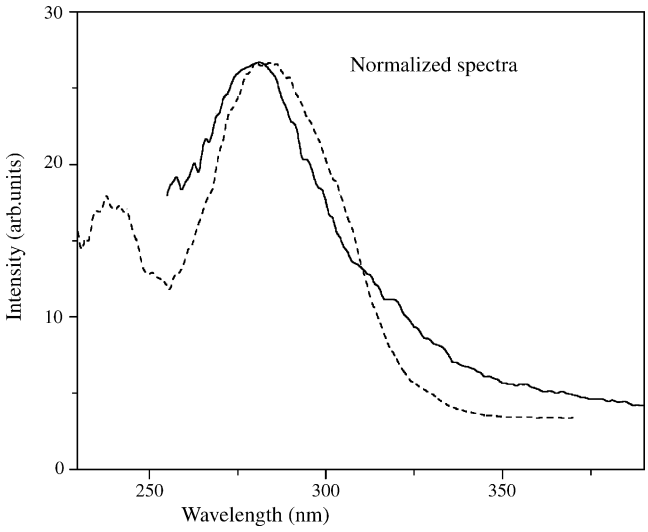

Fig. 4. Fluorescence excitation spectra of 3-APPI in water at pH 5.3 at different emission wavelengths at: (- - -) λ_{em} = 380 nm; (—) λ_{em} = 500 nm.

isolated conditions in S_0 state is MC2 > MC3 > MC1 (0.0, 9.2 and 74.3 kJ mol^{-1}, respectively) and when dipolar solvation energy is included, the order of stability changes to MC1 > MC3 > MC2 (0.0, 18.4 and 45 kJ mol^{-1}, respectively). This is because μ_g of these MCs is 19.0, 2.1 and 10.8 D in order of MC1–MC3. In other words, formation of MC2 is more favorable in non-polar solvents and that of MC1 in polar protic ones. Similarly charge density data on these three basic centers (N^2:N^8:N^{13} :: 5.231:5.317:5.278) also suggest that the first site of protonation will be $=N^8-$ followed by N^{13} in S_0 state. We have also calculated the global minima at these basic centers, using potential energy mapping program [13]. This method considers the charge densities at a particular basic center of interest plus the effective charges of rest of the atoms in the molecule. Greater the depth of potential well, greater will be the chances of protonation on that basic center. Results indicate that the site $=N^8-$ (MC2) is more reactive (−101.0 kJ mol^{-1}) than the site $=N^2-$ (MC3, −50.5 kJ mol^{-1}). Predictions by the electrostatic mapping are also similar to those by AM1 calculations under isolated conditions and may also agree when solvation energy is included in electrostatic mapping program. Thus it may be concluded that MC2 is more favorable in non-polar solvents and MC1 in polar protic solvents. On the other hand in S_0 state and under isolated conditions, DFT calculations predict MC3 to be more stable than MC2 and MC1 by 29.7 and 120.5 kJ mol^{-1}, respectively. Relative dipole moments of these MCs observed by DFT, also suggests that MC1 will be stable in polar medium. In other words, both these models predict that MC1 is the most stable species in polar medium, whereas AM1 predicts MC2 and DFT predicts MC3 to be the species in non-polar solvents.

Based on the above discussion, the experimental results can be explained as follows. (i) Large red shift observed in the absorption and fluorescence spectra of neutral species in aqueous medium is consistent with the protonation of $=N^2-$ (MC3) rather than $=N^8-$ (MC2) atom. This is because the spectral characteristics of MC formed by protonating $=N^8-$ imidazole ring in BIs are nearly similar to those of neutral species if π, π^* is the lowest energy transition [14]. Large red shift observed in the emission spectrum of neutral species on protonation could also be assigned to MC2, if charge transfer is the lowest emitting state. But the formation of MC2 in aqueous medium can be rejected on the ground that emission band maximum of this species should be sensitive to solvent polarity, whereas in our case it is not. Fluorescence excitation band maximum (350 nm) observed at $\lambda_{em} > 500$ nm, as well as, the emission band maximum (∼460 nm) at $\lambda_{exc} > 320$ nm are the spectral characteristics due to MC3. (ii) Structured blue shifted fluorescence spectrum present in the similar acidic protic systems is assigned to MC1, as the spectral characteristics of the neutral species are blue shifted on protonation of $-NH_2$ group [14]. We could not find out from literature about the spectral characteristics of 2-phenylpyrido[3,4-d]imidazole (PPI), because the spectral characteristics of the MC1 of 3-APPI should be similar to PPI. Fluorescence excitation spectrum (306 nm) observed at $\lambda_{em} < 400$ nm and florescence spectrum (∼330 nm) observed at $\lambda_{exc} \leq 300$ nm confirm the formation of MC1. (iii) Disagreement between the absorption spectrum and the fluorescence excitation spectrum is because of the fact that the latter reflect the absorption spectrum of individual species, whereas the former is a composite absorption spectrum of both the species. (iv) Behavior of MC1 of 3-APPI is quite different from that of MC1 of DMAPPI [27] in the sense that excited state intramolecular proton transfer (ESIPT) involving solvent molecules is not observed in the former. Although $-NH_3^+$ ($-N^+HMe_2$) becomes stronger acid in S_1 [27–33,59–63], and $=N-$ becomes stronger base on excitation, ESIPT of the second kind should have occurred. The absence of this behavior may be due to shorter lifetime of MC1 of 3-APPI and thus cannot compete with protonation or deprotonation rate constants of the respective acid–base conjugate pair. This is supported by the ground state pK_a value obtained from fluorimetric titrations. (v) Assignment of MC3 is further supported by the results of ether + TFA, i.e., only one large red shifted emission at ∼462 nm, invariant of emission spectrum at 462 nm to λ_{exc} in the range of 290–340 nm, only one kind of λ_{max}^{exc} at 345 nm when monitored at $\lambda_{em} > 450$ nm and single exponential decay observed in the emission spectrum.

Thus it may be concluded that MC1 and MC3 are the MCs of 3-APPI present in polar aprotic and polar protic solvents and only MC3 in ether containing TFA.

4.2.3. Dications

In the pH range of 5.4 and 1.0, LW λ_{max}^{ab} (∼340 nm) disappears and SW λ_{max}^{ab} is slightly blue shifted to 286 nm from 292 nm, with isosbestic points at 265 and 305 nm, thus suggesting equilibrium between MCs and DCs. Similar behavior is also observed in acetonitrile and methanol as solvents at H_2SO_4 concentration $\geq 10^{-4}$ M. Relevant data are compiled in Tables 4 and 5. The absorption spectra at pH 5.3, pH 1,

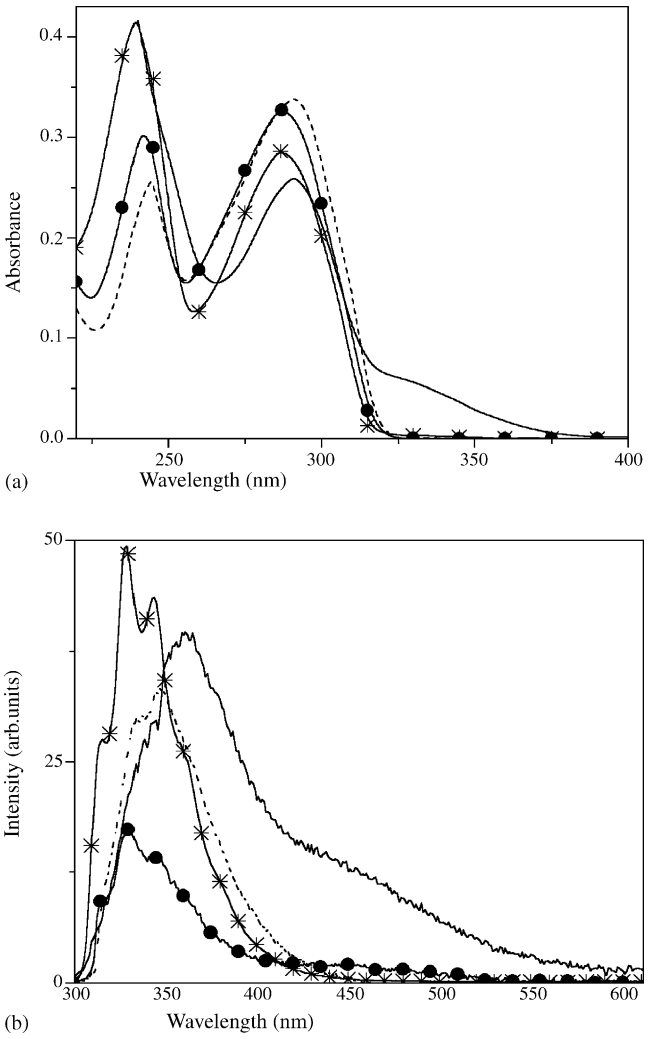

Fig. 5. (a) Absorption spectra of 3-APPI in water at different acid concentrations: (—) pH 5.3; (*) pH 1.0; (●) $H_0 = -3.5$; (- - -) $H_0 = -10$. (b) Fluorescence spectra of 3-APPI in water at different acid concentrations: (—) pH 5.3 (intensity enhanced 30 times); (*) pH 1.55; (●) $H_0 = -2$ (intensity enhanced 10 times); (- - -) $H_0 = -10$ (intensity enhanced 6 times), at $\lambda_{exc} = 305$ nm.

$H_0 = -3.5$ and $H_0 = -10$ are depicted in Fig. 5a. pK_a value obtained for the DC–MC equilibrium from absorption data is found to be 3.30 and given in Scheme 2.

Dual fluorescence spectrum of MC, in the pH range of 5.3 and 1.0 develops in to one structured slightly blue shifted emission ($\nu_{vib} = 1330\ cm^{-1}$) and its intensity increases up to pH 1.0 (Fig. 5a and b). Similar behavior is also observed in acetonitrile and methanol up to 10^{-2} M H_2SO_4. Fluorescence decay profile at pH 1.0 follows a single exponential with lifetime of 0.7 ns. Unlike the MCs, fluorescence band maximum and fluorescence quantum yield is independent of λ_{exc} in the range of 285–315 nm, suggesting that emission is occurring from the most relaxed excited state. Fluorescence excitation spectra recorded at λ_{em} in the range of 330–400 nm and at pH 1.0 resemble with each other and also with the absorption spectrum. This indicates that there is only one species in the S_0 state and emitting and absorbing species are the same.

Similar to MCs there can be three (DC1–DC3, Scheme 1). Results of Table 2 clearly suggest that DC3 is the most unstable DC by 65.2 kJ mol^{-1} under isolated conditions as compared to DC2 and by 62.9 kJ mol^{-1} as compared to DC1 when dipolar solvation energy is included. In other words presence of DC3 is neglected. Under isolated conditions DC2 is stable as compared to DC1 by 62.6 kJ mol^{-1} and DC1 is stable than DC2 by 28.15 kJ mol^{-1} when dipolar solvation is included. DFT theory also predicts that DC2 is the most stable ionic species under isolated conditions. Based on the value of μ_g, it will be clear that DC1 will be the most stable when dipolar solvation energy will be included. In other words no definite conclusion can be drawn from theoretical calculations, but based on the experimental results and other information from Table 2, it may be concluded that DC2 is the only dicationic species present in the system. (i) Absorption transition energy predicted by CNDO/S-CI, as well as, by TD (DFT) agrees with the absorption spectrum for DC2 only, whereas for other species, the discrepancy is quite large. (ii) Geometric optimization in S_1 state, after taking into account the configuration interactions predict that DC3 is the most stable species in S_1 state, but it can be rejected on the ground that emission transition predicted by AM1 method is way off from the experimental results. (iii) MC1 and MC3 are the monocationic species formed in S_0 state, as mentioned above. Further protonation of MC1 will lead to red shift, whereas that of MC3 will give rise to blue shift in the spectral characteristics. Results are consistent with the above explanation. (iv) Single emission band, invariance of fluorescence band maximum on λ_{exc} and fluorescence excitation spectrum on λ_{em}, resemblance of fluorescence excitation with absorption spectrum and single lifetime confirms the presence of only one species and that is DC2.

4.2.4. Trications

With further increase of acid strength up to $H_0 = -3.5$, LW λ^{ab}_{max} at 286 nm is slightly red shifted to 290 nm with small increase of absorbance, whereas SW λ^{ab}_{max} is red shifted from 239 to 244 nm, with large decrease of absorbance, such that the absorbance of two bands is reversed (Fig. 5a). LW λ^{ab}_{max} of this species of 3-APPI resembles with the trication (TC) of DMAPPI (∼290 nm) [27]. Except the position of amino group on the phenyl ring, basic aromatic ring of both 3-APPI and DMAPPI are the same and thus absorption characteristics of the TC of both the molecules should be nearly similar. No change is observed in absorption spectra with further increase of acid strength up to $H_0 = -10.0$. Decrease of fluorescence intensity of the structured emission with increase of acid concentration supports the protonation of $=N^8-$ atom. This is because Φ_f of such protonated species is nearly 1/10 of the neutral species [14]. Increase of fluorescence intensity at $H_0 < -3$ could be due to dielectric effect of the solvent (Fig. 5b). A similar behavior has been observed in 9,10-phenanthroimidazole [62] and carbonyl groups of

carboxylic acid group and amide group [63] prior to the protonation. A similar behavior in emission spectrum of DC2 is also observed in acetonitrile and methanol at $[H_2SO_4] > 10^{-2}$ M, with the exception, that no new emission band is observed. This is because sulphuric acid concentration in these solvents was not large enough in these solvents. Similarity of fluorescence excitation spectra recorded at different λ_{em} with the absorption spectrum at $H_0 = -10$ confirms the presence only one TC, formed by protonating $=N^2-$, $=N^8-$ and $-NH_2$ atoms. pK_a value determined form absorption data is found to be −1.0. Excited state pK_a value for TC–DC could not be determined because the fluorescence intensity of TC did not reach a saturation point.

5. Conclusions

On the basis of absorption, fluorescence excitation and fluorescence spectroscopy as well as using time dependent spectrofluorimetry and theoretical calculations, the following conclusions can be drawn: (i) 3-APPI is sensitive to solvent polarity better in S_1 state than in S_0 state and thus can be a good probe molecule. (ii) Only one kind of MA is observed by deprotonating $>$N–H moiety. (iii) MC1 and MC3 are formed in polar aprotic and polar protic solvents, but only MC3 is formed in ether containing TFA. (iv) Only one kind of DC (namely DC2) and TC are formed in both in S_0 and S_1 states.

Acknowledgement

The authors are thankful to the Department of Science and Technology, New Delhi, for financial support under the project number SP/S1/H-07/2000.

References

[1] H.H. Jaffe, M. Orchin, Theory and Applications of Ultraviolet Spectroscopy, Wiley, New York, 1962.
[2] J.F. Ireland, P.A.H. Wyatt, Adv. Phys. Org. Chem. 12 (1976) 132.
[3] S.J. Formosinho, L.G. Arnaut, J. Photochem. Photobiol. A: Chem. 75 (1993) 1.
[4] R. Manoharan, S.K. Dogra, Bull. Chem. Soc. Jpn. 60 (1987) 4401.
[5] R. Manoharan, S.K. Dogra, J. Phys. Chem. 92 (1988) 5282.
[6] A. Paul, R.S. Sarpal, S.K. Dogra, J. Chem. Soc., Faraday Trans. I 86 (1990) 2095.
[7] J.R. Lakowictz, Principles of Fluorescence Spectroscopy, Kluwer Academic Publishers/Plenum Press, New York, 1999.
[8] S.K. Dogra, Proc. Indian Acad. Sci. 104 (1992) 635.
[9] S.K. Dogra, J. Ind. Chem. Soc. 80 (2003) 419.
[10] J.J. Spanget-Larsen, J. Chem. Soc., Perkin Trans. 2 (1985) 417.
[11] J. Waluk, W. Rettig, J.J. Spanget-Larsen, J. Phys. Chem. 92 (1980) 6930.
[12] J.J. Spanget-Larsen, J. Phys. Org. Chem. 8 (1995) 496, and references therein.
[13] P.C. Mishra, B.P. Asthana, Quantum chemistry, QCPE Bulletin Program No. QCMP039, 7 (1986) 176. Indiana University, Bloomington, IN, USA.
[14] M. Krishnamoorthy, P. Phaniraj, S.K. Dogra, J. Chem. Soc., Perkin Trans. II (1986) 1917;
H.K. Sinha, S.K. Dogra, J. Chem. Soc., Perkin Trans. II (1987) 1465.
[15] A.K. Mishra, M. Swaminathan, S.K. Dogra, J. Photochem. 26 (1984) 947.
[16] S.G. Schulman, A.C. Capomacchia, M.S. Rietta, Anal. Chim. Acta 56 (1971) 91.
[17] F. Rodriguez-Prieto, M. Mosquera, M. Novo, J. Phys. Chem. 94 (1990) 8536.
[18] M.C.R. Rodriguez, J.C. Renedo, R.J. Willemse, M. Mosquera, F. Rodriguez–Prieto, J. Phys. Chem. 103 (1999) 7236.
[19] M. Mosquera, M.C.R. Roderiguez, F. Prieto-Rodriguez, J. Phys. Chem. 101 (1997) 2766.
[20] E. Fasani, A. Albini, P. Savarino, G. Viscardi, E. Barni, J. Heterocycl. Chem. 30 (1993) 1041.
[21] M. Swaminathan, S.K. Dogra, J. Am. Chem. Soc. 105 (1983) 6223;
P. Phaniraj, A.K. Mishra, S.K. Dogra, Indian J. Chem. 24A (1985) 913.
[22] K. Iyer, M. Krishnamoorthy, S.K. Dogra, J. Photochem. 28 (1987) 273;
S. Santra, S.K. Dogra, Chem. Phys. 207 (1996) 103.
[23] S.K. Das, S.K. Dogra, J. Chem. Soc., Perkin Trans. II (1998) 2765.
[24] G. Krishnamoorthy, S.K. Dogra, J. Lumin. 92 (2001) 91, 103.
[25] S. Santra, S.K. Dogra, J. Mol. Struct. 487 (1999) 199.
[26] G. Krishnamoorthy, S.K. Dogra, Spectrochim. Acta A 55 (1999) 2647.
[27] G. Krishnamoorthy, S.K. Dogra, J. Org. Chem. 64 (1999) 6566.
[28] A.K. Mishra, S.K. Dogra, Indian J. Phys. 58B (1984) 480.
[29] A.K. Mishra, S.K. Dogra, J. Photochem. 31 (1985) 333;
S. Santra, S.K. Dogra, Chem. Phys. 226 (1998) 285.
[30] A.K. Mishra, S.K. Dogra, Bull. Chem. Soc. Jpn. 58 (1985) 3587.
[31] J.K. Dey, S.K. Dogra, Chem. Phys. 143 (1990) 97.
[32] J.K. Dey, S.K. Dogra, Bull. Chem. Soc. Jpn. 64 (1991) 3142.
[33] R.W. Middleton, D.G. Wibberely, J. Heterocycl. Chem. 17 (1980) 1757.
[34] M.J. Jorgenson, D.R. Hartter, J. Am. Chem. Soc. 79 (1957) 427.
[35] G. Yagil, J. Phys. Chem. 71 (1967) 1034.
[36] S.R. Meach, D. Phillips, J. Photochem. Photobiol. A: Chem. 23 (1983) 193.
[37] M.K. Nayak, S.K. Dogra, J. Photochem. Photobiol. A: Chem. 161 (2004) 169.
[38] H.H. Hinze, H.H. Jaffe, J. Am. Chem. Soc. 84 (1962) 540.
[39] M.J.S. Dewar, E.G. Zeoblish, E.F. Healy, J.J. Stewart, J. Am. Chem. Soc. 107 (1985) 3902.
[40] J. Delbene, H.H. Jaffe, J. Chem. Phys. 48 (1989) 1807.
[41] A. Kumar, P.C. Mishra, QCPE Bull. 9 (1989) 67.
[42] N. Mataga, T. Kubota, Molecular Interactions and Electronic Spectra, Marcel Dekker, New York, 1970.
[43] E. Lippert, Z. Electrochim. 61 (1957) 962.
[44] M. Head-Gordon, E.S. Replogte, J.A. Pople, Gaussian'98 Revision, Gaussian Inc., Pittsburgh, PA, 1998.
[45] A.D. Becker, J. Chem. Phys. 98 (1993) 5648.
[46] R.G. Parr, W. Yang, Density Functional Theory of Atoms and Molecules, Oxford University Press, New York, 1989.
[47] G.A. Peterson, M.A. Al-Lahan, J. Chem. Phys. 94 (1991) 6081.
[48] J.B. Foresman, A. Frisch, Exploring Chemistry with Electronic Structure Methods, 2nd ed., Gaussian Inc., Pittsburgh, PA, 1996.
[49] J.B. Foresman, M. Head-Gordon, J.A. Pople, M.J. Frisch, J. Phys. Chem. 96 (1992) 135.
[50] M.E. Casido, C. Jamorski, K.C. Casido, D.R. Salahub, J. Chem. Phys. 108 (1998) 439.
[51] A.K. Mishra, S.K. Dogra, Spectrochim. Acta A 39 (1983) 609.
[52] M. Kasha, Discuss. Faraday Soc. 9 (1950) 14.
[53] S.K. Saha, S.K. Dogra, J. Mol. Struct. 470 (1998) 301.
[54] G. Kohler, J. Photochem. 38 (1987) 217.

[55] M. Sow, G. Durrocher, J. Photochem. Photobiol. A: Chem. 59 (1990) 349.
[56] E. Lippert, Z. Naturforsch. 10A (1955) 541;
E. Lippert, Z. Naturforsch. 17A (1962) 621.
[57] N. Mataga, Y. Kaife, M. Koizumi, Bull. Chem. Soc. Jpn. 28 (1955) 690.
[58] S. Mazumdar, R. Manoharan, S.K. Dogra, J. Photochem. Photobiol. A: Chem. 46 (1989) 301.
[59] S.K. Saha, S.K. Dogra, J. Photochem. Photobiol. A: Chem. 110 (1997) 257.
[60] A.K. Mishra, S.K. Dogra, Indian J. Chem. 24A (1985) 285.
[61] H.K. Sinha, S.K. Dogra, J. Photochem. 36 (1987) 149.
[62] M. Swaminathan, S.K. Dogra, J. Chem. Soc., Perkin Trans. II (1983) 1641.
[63] R. Manoharan, S.K. Dogra, J. Photochem. Photobiol. A: Chem. 50 (1989) 53.